

# Role of MRI Diffusion in Evaluation the Therapeutic Response and Prognostic Outcome in Pediatric Patients with Rhabdomyosarcoma

Rehab Ibraheem <sup>a</sup>, Medhat Refaat <sup>a</sup>, Inas M. El-nadi <sup>b</sup>, Tarek A. Raafat <sup>c</sup>

<sup>a</sup> Department of Radiodiagnosis, Faculty of Medicine, Benha University, Egypt.

<sup>b</sup> Department of oncology medicine, Faculty of Medicine, Benisuef University, Egypt.

<sup>c</sup> department of diagnostic radiology, national cancer institute, Cairo, Egypt.

**Correspondence to:** Rehab Ibraheem, Department of Radiodiagnosis, Faculty of Medicine, Benha University, Egypt

**Email:**

rehabhussein13@gmail.com

**Received:** 6 July 2021

**Accepted:** 15 February 2021

## Abstract

**Background:** Childhood rhabdomyosarcoma accounts for about 3.5% of cancer cases among children (0 to 14 years of age). The most common sites are the head and neck. Early detection of treatment response might change therapeutic strategies and unnecessary toxicity might be avoided. The differentiation between post-therapeutic changes and recurrent tumors in RMS is a diagnostic dilemma. DWI helps predict and monitor treatment response in RMS, as changes in ADC precede changes in tumor size. For the differentiation between recurrent tumor and post-therapeutic changes, qualitative and quantitative assessment using DWI seems to be helpful. **Purpose:** assess the accuracy of DW-MRI in evaluation, monitoring the treatment response in RMS and differentiation between recurrent tumor and post-therapeutic changes. **Data Sources:** Previous literature, reviews, and studies as well as medical websites (PubMed, radiographic and Science Direct) and scientific journals databases were searched from the start date of each database. **Patients and methods:** During the period between April 2017 to April 2019, 40 pediatric patients with rhabdomyosarcoma (24 male and 16 female) were enrolled prospectively. All patients underwent standard MRI protocol and DW-MRI. PET/CT was done and correlated to SUV/MAX value with the DWI results. **Results:** Correlation between DW-MRI and PET/CT showing 100 % sensitivity and 82.14 % specificity with 87.50 % accuracy in differentiation between recurrent tumor and post-therapeutic changes. **Conclusion:** The DW-MRI allows accurate characterization of rhabdomyosarcoma, assessment of treatment response, and differentiation between recurrent tumor and post-therapeutic changes.

**Keywords:** DW-MRI, pediatric, rhabdomyosarcoma.

## **Introduction:**

Childhood rhabdomyosarcoma (RMS) accounts for approximately 3.5% of cancer cases among children (0 to 14 years of age) (1). RMS arises from skeletal muscle progenitor cells and can occur anywhere in the body irrespective of striated muscle content. The most common sites of RMS in children are the head and neck (2).

Three main groups of RMS are recognized, based on histological morphology: embryonal, alveolar, and pleomorphic, of which the former two mainly occur in children and the latter only in adults. The embryonal type of RMS (eRMS) accounts for about 70% of cases, affecting younger patients with better prognosis. Alveolar RMS accounts for about 15% and is seen in older children with worse prognosis (3). Most head and neck RMS are solitary, unilateral bulky lesions, although multifocal RMS has been reported (4).

Early detection of treatment response might change therapeutic strategies in non-responders, whereby unnecessary toxicity and negative side effects might be avoided and individualized treatment would be possible with an ultimate goal of increasing long-term survival and saving money by

avoiding ineffective treatment (4). Differentiation of tumor recurrence or metastases from post-therapeutic signal alteration can be challenging, using standard MR imaging techniques (5).

The differentiation between post-therapeutic changes and recurrent tumors in patients treated for RMS is a diagnostic dilemma both for the radiologists and the clinicians. These diagnostic problems are because chemotherapy and radiotherapy may lead to extensive changes of the underlying tissue including soft-tissue edema, cartilage necrosis, fibrosis, and perichondritis (6).

DWI helps predict and monitor treatment response in RMS, as changes in ADC precede changes in tumor size. An increase in ADC early after initiation of treatment without any decrease during treatment is correlated with good response (7). DWI might allow prediction of outcomes at an early point and might therefore help individualize treatment. For the differentiation between recurrent tumor and post-therapeutic changes, qualitative and quantitative assessment using DWI seems to help resolve this diagnostic dilemma (8).

The purpose of this study is to assess the diagnostic accuracy of diffusion MRI in evaluating and monitoring treatment response in RMS as well as differentiating between recurrent tumor and post-therapeutic changes.

## **Materials and methods**

### **Population**

This prospective study was performed during the period from April 2017 to April 2019. It included 40 pediatric patients with rhabdomyosarcoma. Patients were selected from a series of patients with RMS who have been followed in Cancer Children Hospital 57357.

### **Ethical committee approval:**

Ethical approval for this study was obtained from our institutional review board and written informed consent for publication of this work was provided by the patients' guardians at the time of admission, as per the hospital's policy.

### **STUDY METHODS:**

- The population of study & disease condition: Pediatric patients (up to 18 years) with pathologically proven RMS

### **Inclusion criteria**

- Patients had initial and follow-up MRI and PET /CT.
- Pathological proven RMS.

### **Exclusion criteria**

- No pathological correlation.
- Known patient with RMS had no MRI or PET/CT available
- Patients with bad general conditions and patients with contraindications to MRI or general anesthesia.

Patients included in the study were subjected to full history taking, clinical examination, laboratory investigations, histopathological examination, MRI, and PET/CT examination.

### **Methods**

All patients included in this study underwent DW-MRI was followed by contrast-enhanced MRI.

Patients were examined with 1.5 T scanner (Siemens) in supine position with the most optimal surface coil to accommodate each lesion.

Patients undergone MRI and PET/CT examination initially before treatment and were followed-up for 18 months after initiation of treatment.

## 1- MR Diffusion Imaging

In cases of **head and neck RMS**, diffusion-weighted MR imaging was obtained using a multi-section single-shot echo-planar imaging sequence (TR/TE/NEX: 2200/139 ms/1) field of view 195-400 mm, matrix size 128x128, slice thickness 4-7 mm, section gap 0.3 mm with b values of 0 and 1000 s/mm<sup>2</sup>.

In cases of **pelvis RMS**, diffusion-weighted MR imaging was obtained using a multi-section single-shot echo-planar imaging sequence (TR/TE/NEX > 3500 ms/1) field of view 240-280 mm, matrix size 128x128, slice thickness 4-7 mm, section gap 1-2 mm with b values of 0, 100 and 800 s/mm<sup>2</sup>.

In cases of **extremity RMS**, diffusion-weighted MR imaging was obtained using a multi-section single-shot echo-planar imaging sequence (TR/TE/NEX > 1500/80 ms/1) field of view 180-250 mm, matrix size 256x256, slice thickness 1-4 mm, section gap 1-2 mm with b values of 0, 100 and 800 s/mm<sup>2</sup>.

The signal intensities of the lesion on DWI were classified as hypointense (free diffusion) or hyperintense (restricted diffusion).

The ADC maps were calculated automatically by the MRI software. Measurements of ADC value were made in

different regions of interest (ROI) within the lesions and the mean ADC value was calculated. The ADC values were expressed in mm<sup>2</sup>/s.

The ADC was measured by manually placing regions of interest in tumor regions on the ADC map. In the solid lesions, regions of interest were placed at the site of enhancing parts on contrast-enhanced T1-weighted MR images.

We compared the ADC maps and other MR images carefully and placed the regions of interest only in the solid tumor components excluding the cystic, necrotic, and hemorrhagic tumor areas. We chose regions of interest as central as possible within the tumor area at random and averaged the ADC of each tumor.

## 2- Conventional contrast enhanced MRI (CE-MRI)

Each lesion using the following sequences:

- Scout T1 TFE.
- Axial and coronal T1 weighted fast spin echo.
- Axial and coronal T2 weighted fast spin echo.
- Axial T2 fat-suppressed fast spin-echo.
- After intravenous administration of gadolinium DTPA (0.3 mg/kg),

contrast-enhanced axial, sagittal, and coronal T1WIs are obtained.

The lesions were evaluated in MRI as follows:

- The number of lesions.
- Signal behavior on T1 & T2 (iso, hypo, and hyperintense relative to muscles)
- Presence of intra-tumoral hemorrhagic or necrotic components.
- Enhancement degree (no, minimal or avid) and pattern (homogenous or heterogeneous).

### **PET/CT correlation**

PET/CT was done and correlate the SUV/MAX value with the DWI results.

### **Statistical analysis**

Data were coded and entered using the statistical package for the Social Sciences (SPSS) version 26 (IBM Corp., Armonk, NY, USA). Data was summarized using mean, standard deviation, median, minimum and maximum in quantitative data and using frequency (count) and relative frequency (percentage) for categorical data.

### **Results:**

The current study included 40 pediatric patients with RMS, their ages at the time of the study ranged between 10 months to 15 years. Male patients represented 60%, while

female patients represented 40% of the total examined cases (24 male and 16 female). The head and neck are the seats of more than 72 %.

Based on the MRI pattern; most of the lesions (54.7%) were ill-defined, 94.1% had an irregular outline, and 50.2% invading the adjacent structures. The lesions elicit a low T1 signal in 82.8% of cases and a high T2 signal in 66.5% of cases. In contrast, enhanced MRI; 79.3% of the lesions presented heterogeneous enhancement, 16.7% presented homogenous enhancement, 1% presented rim enhancement, while 3% presented no enhancement. In diffusion MRI; 28.9% of cases were hyperintense, 29.4% were hypointense, 9.6% were isointense while 32% presented mixed signals.

The calculated ADC values of the lesions ranged from 0.30 to 2.8 x 10<sup>-3</sup> mm<sup>2</sup>/sec with a mean value of 1.5x10<sup>-3</sup> mm<sup>2</sup>/sec. The calculated SUV/MAX values of the lesions ranged from 0.90 to 10.90 with a mean value of 4.06 (Table 1).

Regarding the PET/CT, 38.5% of the cases presented active uptake while 61.5% presented non-active uptake.

PET/CT showed good response to treatment with no residual lesions in 70 % of cases (28

out of 40 patients), non-active uptake. While, it showed a poor response to treatment with residual lesions in 30 % of cases (12 out of 40 patients), active uptake with mean SUV/MAX 2.97. P-value was about 0.829 (Table 2).

By diffusion MRI, 57.5 % of the cases (23 out of 40 patients) showed good response to treatment, and mean ADC measured  $2.24 \times 10^{-3}$  mm<sup>2</sup>/sec. While 42.5 % of cases (17 out of 40 patients) showed poor response to treatment with restricted diffusion. The cut-off average ADC value for detecting recurrent/ residual lesions was  $\leq 1.82 \times 10^{-3}$  mm<sup>2</sup>/sec. P-value was about 0.060 (Table 3).

The lesions that showed good response represents facilitated diffusion (hypointense signal) in 47.8% and restricted diffusion (hyperintense signal) in 23.2%. While the lesions that showed poor response represents restricted diffusion (hyperintense signal) in 38.9% of cases and facilitated diffusion (hypointense signal) in 19.9% of cases.

One of the pitfalls of DWI is the mixed signal of the lesions. In our study, the lesions with good responses represented the mixed signal in 29.0% of cases. While the lesions with poor response represented a mixed signal in 41.2% of cases.

In comparison between MR findings & PET/CT findings, we found:

- All residual lesions that show active uptake in PET/CT, showed diffusion restriction in DWI, and represent 12 cases (100 %).
- Five (17.9 %) cases showed no residual lesion in PET/CT (non-active uptake) but showed diffusion restriction in DWI. They represent the false-positive result of DWI.
- Twenty three cases (82.1%) had a good response and no residual lesion in DWI (facilitated diffusion) showed non-active uptake in PET/CT.
- No reported cases showing active uptake in PET/CT and facilitated diffusion in DWI.

By correlation between the DWI results and PET/CT for detection of the residual lesion, the DWI showed a sensitivity of 100 % and specificity of 82.14 % with an accuracy of 87.50 %.

Considering all lesions included in the study, a strong inverse correlation was found between SUV MAX and ADC values (correlation coefficient  $r=-0.520$ ,  $p<0.001$ ).

**Table.1:** Calculated ADC and SUV/MAX.

	Mean	Standard Deviation	Minimum	Maximum
Age (Years)	5.64	3.83	0.90	15.00
ADC value	1.50	0.68	0.30	2.80
SUV/MAX	4.06	2.29	0.90	10.90

**Table 2:** Calculated SUV/MAX value in poor prognosis.

	poor					P value
	Mean	SD	Median	Minimum	Maximum	
SUV/MAX	2.97	1.70	2.30	1.50	6.70	.829

**Table 3:** Calculated ADC value in good and poor prognosis.

	Response		
	poor	good	
ADC value	Mean	1.82	2.24
	Standard	0.50	0.95
	Minimum	0.60	1.00
	Maximum	3.00	5.20

## Discussion:

Rhabdomyosarcoma (RMS) is the most common malignant soft-tissue sarcoma in children (v). Head and neck rhabdomyosarcoma (HNRMS) comprises 40% of all RMS and are the most common regions of primary tumor sites (A).

According to its pathological features, RMS is categorized into embryonal RMS (ERMS), alveolar RMS (ARMS),

pleomorphic RMS (PRMS), and fusiform/sclerosing RMS. Among these, ERMS is the most common type in children, accounting for 65% to 80% of all children with RMS (4).

Owing to its contrast resolution, MRI is the modality of choice for the evaluation and characterization of soft-tissue sarcomas, which are achieved by combining

conventional and advanced multiparametric MRI (10).

Conventional MRI techniques can demonstrate tumor composition, extent, compartmental involvement, and relationship with other structures for accurate treatment planning before surgery. However, conventional techniques remain inadequate for differentiation of malignant from benign lesions owing to overlap in the signal intensity characteristics of these tumors and are also limited in the assessment of residual or recurrent disease after treatment. The surgical bed is often associated with heterogeneous signal intensity and scar tissue that can potentially obscure a recurrence (11).

Multiparametric or functional MRI, which includes techniques such as diffusion-weighted imaging (DWI), can allow more accurate characterization of malignancy, assessment of treatment response, and evaluation of postsurgical residual or recurrent disease (10). Mean apparent diffusion coefficient (ADC) values may help differentiate benign and malignant lesions, whereas changes in ADC tumor heterogeneity evaluated longitudinally during treatment may provide another method of characterizing tumor viability (12).

It has been shown that there is an inverse correlation between cellular density and ADC, describing a high cellular density as a low ADC-value due to high restriction in tissue and hereby decreased water movement. Accordingly, it has been shown that in general there is an increase in ADC-value following effective treatment. (13).

Our prospective study protocol was reviewed and approved by the institutional review board of our hospital. This study enrolled 40 pediatric patients with RMS. The collected cohorts of patients undergone MRI DWI assessments and full ascertainment of outcomes, potentially comparing their predictive value to PET-CT, to produce an effective evaluation of this advanced functional imaging technology in this indication.

The purpose of this study is to assess the diagnostic accuracy of diffusion MRI in the evaluation and monitoring of the treatment response in RMS as well as differentiation between recurrent tumor and post-therapeutic changes. In this study, the tumors were assessed qualitatively and quantitatively by the measurement of ADC values.

MRI examinations were performed with an MRI scanner at Cancer Children Hospital 57357 using a 1.5 T scanner. Most of the



patients in our study manifest as local painless lumps and lump-related oppression. All the cases were examined in a supine position with the most optimal surface coil to accommodate each lesion.

In our study, the male/female ratio was 24:16 which shows male predominance, this is going with **Meng Li, et al.** (14) as they also showed male predominance among demographic information of 40 cases with RMS showing male/female ratio 22:18.

The ages of the patients in our study ranged between 10 months to 15 years with a mean age of 5.64 years, in **Meng Li, et al.** (14) the patients' age ranged from 3 months to 17 years with a median age of 5.21 years.

In our study, most of the lesions were in the head and neck region (29 cases accounting for 72.5%) other sites include the lower limbs (1 case accounting for 2.5%), upper limbs (1 case accounting for 2.5%), and the pelvis (9 cases accounting for 22.5%). However, in **Meng Li, et al.** (14) study, the primary onset sites in 9 patients were the limbs and in 3 patients the mediastinum, accounting for 22.5% and 7.5%, respectively, indicating that RMS may occur in any part of the body with striated muscle cell-like tissues.

In our study, based on MRI pattern, most of the lesions (54.7%) were ill-defined, 94.1%

irregular outline and 50.2% invade the adjacent structures. The lesions elicit low T1 signal in 82.8% of cases, high T2 signal in 66.5% and heterogeneous contrast enhancement in 79.3% of cases.

This is going with **Kim, et al.** (15) who reported that most tumors had a poorly defined margin (81.2%) and heterogeneous enhancement (91.3%). Necrosis and local invasion were observed in (46.4%) and (65.2%) patients, respectively.

In this study b values (0, 800, and 1000 s/mm<sup>2</sup>) in three orthogonal directions lead to adequate background suppression and damping of the signal given by cystic necrosis in malignant lesions. This is also supported by **Khoo, et al.** (16) who reported recommendations that emphasize the importance of using three b values instead of two to obtain accurate ADC values.

In our study, by diffusion MRI 28.9% of the lesions appeared hyperintense (restricted), 29.4% hypointense, 9.6% isointense while 32% presented mixed signal.

This is going with **Kumar Y, et al.** (17) who reported increased restricted diffusion in high-grade malignancies, which is also related to a high nucleocytoplasmic ratio in rapidly proliferating tumors, as there is the higher restriction of water molecules in the nucleus in comparison to the cytoplasm.

**Albalawi, et al.** (18) reported that 60% of lesions showed high signal intensity on DWI, 26.7% showed low signal intensity, and 13.3% of cases showed mixed signal intensity.

In this study, the highest observed ADC of the lesions was  $2.8 \times 10^{-3} \text{ mm}^2/\text{s}$  while the lowest ADC was  $0.30 \times 10^{-3} \text{ mm}^2/\text{s}$ . The mean ADC value was  $1.5 \times 10^{-3} \text{ mm}^2/\text{s}$ . This differs from **Gill Norman, et al.** (19) who showed the range of mean ADCs reported for RMS was 0.78 to  $1.21 \times 10^{-3} \text{ mm}^2/\text{s}$ . It also differs from **Albalawi, et al.** (18) who showed the range of mean ADCs reported for RMS was 0.67 to  $0.09 \times 10^{-3} \text{ mm}^2/\text{s}$ .

This variation was explained by **Humphries, et al.** (20) who claimed it was due to differences in tumor cellularity and extracellular stromal density. Also, cellular size and cytoplasmic nuclear ratio play a role.

One of the challenges that must be faced to enable widespread use of ADC measurement in clinical practice is the stabilization of study methods and reporting. Comparing the results of this study with others was sometimes confusing due to differences in imaging sequences and differences in b-values.

The development of organ-specific guidelines for DWI acquisition, ADC

measurement and checklists for reporting results may facilitate the comparison of study results and contribute to the implementation of ADC measurement for the tumor characterization in the clinical setting (21).

In our study, according to DWI and ADC values, we found residual lesions in 17 out of 40 patients (42.5%). Most of the residual lesions showing mixed signals at DWI (41%), while 38.9% appear hyperintense and 19.9% appear hypointense. The ADC values of recurrent sarcomas were significantly different from those of postoperative scars.

The cut-off average ADC value for detecting recurrent/ residual lesions was  $\leq 1.82 \times 10^{-3} \text{ mm}^2/\text{sec}$  with P-value about 0.060. This is significantly different from those of post-therapeutic changes (average ADC value was  $\geq 2.62 \times 10^{-3} \text{ mm}^2/\text{sec}$ ).

According to the PET/CT result, we found 12 out of 40 cases (30 %) showing residual lesions and representing active uptake with mean SUV/MAX was 2.97 and P-value about 0.829.

It means there were 5 cases (17.9 %) that showed no residual lesions in PET/CT (non-active uptake) but had diffusion restriction in DWI which represent false-positive results in DWI.

Our study includes a case of 2 years male patient with left petrous rhabdomyosarcoma (Fig. 1) showing residual lesion after treatment with ADC value measures  $1.67 \times 10^{-3} \text{ mm}^2/\text{s}$  and final PET/CT shows active uptake with SUV/MAX was 2.9.

**Hassold, et al.** (۲۲) have reported a case of orbital RMS where low ADC value within the recurrent tumor ( $0.62 \times 10^{-3} \text{ mm}^2/\text{s}$ ) helped to differentiate it from post-therapeutic changes.

This is comparable to another study (۲۳) as in they showed that 6 out of 37 patients (16.2 %) had residual lesions and 31 out of 37 patients (83.8 %) didn't have residual lesions. The quantitative ADC measures of recurrent disease ( $1.08 \times 10^{-3} \text{ mm}^2/\text{s}$ ) were significantly different than those of mass-like areas of enhancement without recurrence (postoperative fibrosis) ( $1.9 \times 10^{-3} \text{ mm}^2/\text{s}$ ) or hematomas ( $2.34 \times 10^{-3} \text{ mm}^2/\text{s}$ ).

In our study, according to DWI and ADC values the lesions that showed good response to treatment represent about 75.5 % (23 out of 40 patients), they represented facilitated diffusion (hypointense signal) in 47.8%, restricted diffusion (hyperintense signal) in 23.2% and mixed-signal 29.0%. with mean ADC measures  $2.24 \times 10^{-3} \text{ mm}^2/\text{sec}$ .

According to the PET/CT result, we found 28 out of 40 cases (70 %) showing a good response to treatment with no residual lesion (non-active uptake).

All cases that have a good response with no residual lesions in DWI also showed non-active uptake in PET/CT.

Our study also includes a case of 7 years male patient with left infratemporal rhabdomyosarcoma (Fig. 2) showing good therapeutic response with ADC value measures  $2.1 \times 10^{-3} \text{ mm}^2/\text{s}$  after treatment consistent with post-therapeutic changes and final PET/CT shows no uptake.

Our results showed high sensitivity of DWI and ADC value (100 %) yet lower specificity (82.14 %) with an accuracy of 87.50 %.

However, static post-contrast T1-weighted MR imaging had low specificity because of mass-like enhancement which was observed in many cases without recurrence (13 out of 40 patients with benign post-therapeutic changes).

A study by **Del Grande, et al.** (۲۳) concluded that diffusion-weighted (DW) imaging with apparent diffusion coefficient (ADC) mapping offers increased specificity (97%) in the differentiation of tumor recurrence from postoperative inflammation

and fibrosis; however, it was not sensitive (60%).

However, DW imaging is usually associated with more artifacts than conventional sequences and offers a lower signal-to-noise ratio giving DW imaging lower quality than conventional sequences. Therefore, it is likely that a small lesion will be more difficult to diagnose with DW imaging than with conventional sequences (٢٣).

In our study, the ADC map performance was comparable to PET/CT in detecting small recurrent/residual lesions within the surgical bed, they were accurately depicted as low signal intensity within the surgical bed at the ADC map and active uptake at PET/CT.

**Ashkan A, et al.** (٢٤) reported one of the pitfalls of visual assessment of DWI is that an area with a very long T2 relaxation time may remain high signal and be mistaken for restricted diffusion. This false impression was corrected in the ADC image. Thus, ADC proved to be much more accurate in judging lesions.

In conclusion, our study results showed that the DW imaging and ADC add a significant value in the characterization of postoperative signal abnormalities and recurrence detection because these sequences offered increased sensitivity and specificity for differentiating recurrent tumors from scar tissue.

However, our study showed some limited value of the use of DW imaging with ADC in 5 cases in which post-therapeutic changes mimic the residual lesions while showing no active uptake at PET/CT and was representing false-positive results of DWI.

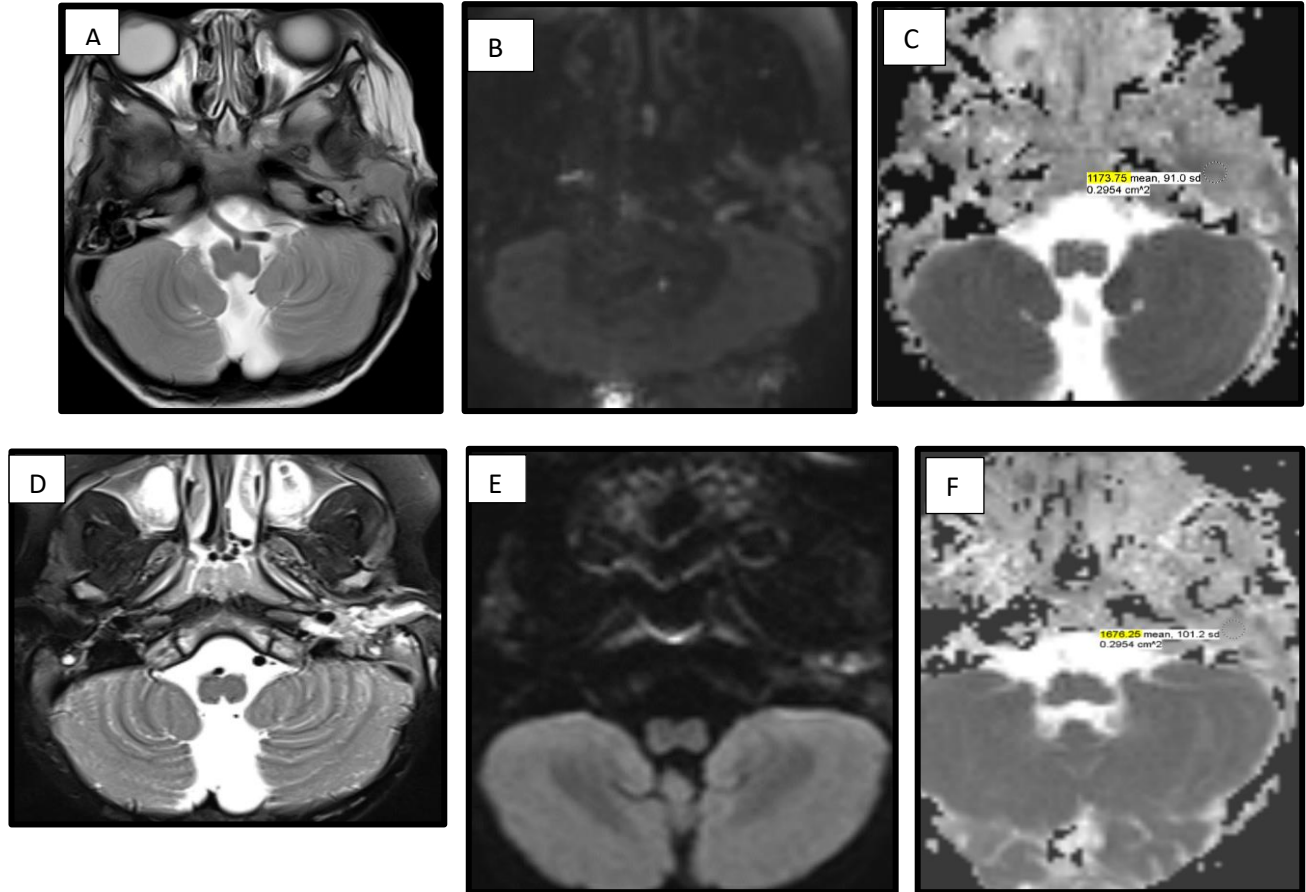


**Fig. 1: Left middle ear Rhabdomyosarcoma in a 2-year-old male.**

- A. axial T2, B. axial MR DWI and C. ADC map images obtained prior to treatment show left petrous mass of low signal intensity that corresponds to a cellular tumor with ADC values of  $1.17 \times 10^{-3} \text{ mm}^2 / \text{sec}$ .
- D. axial T2, E. axial MR DWI and F. ADC map images obtained following treatment show a decrease in tumor size and increase in signal heterogeneity with ADC values of  $1.67 \times 10^{-3} \text{ mm}^2$ . Corresponding with residual lesion.
- The final PET/CT results show mild uptake with SUV/MAX 2.9.

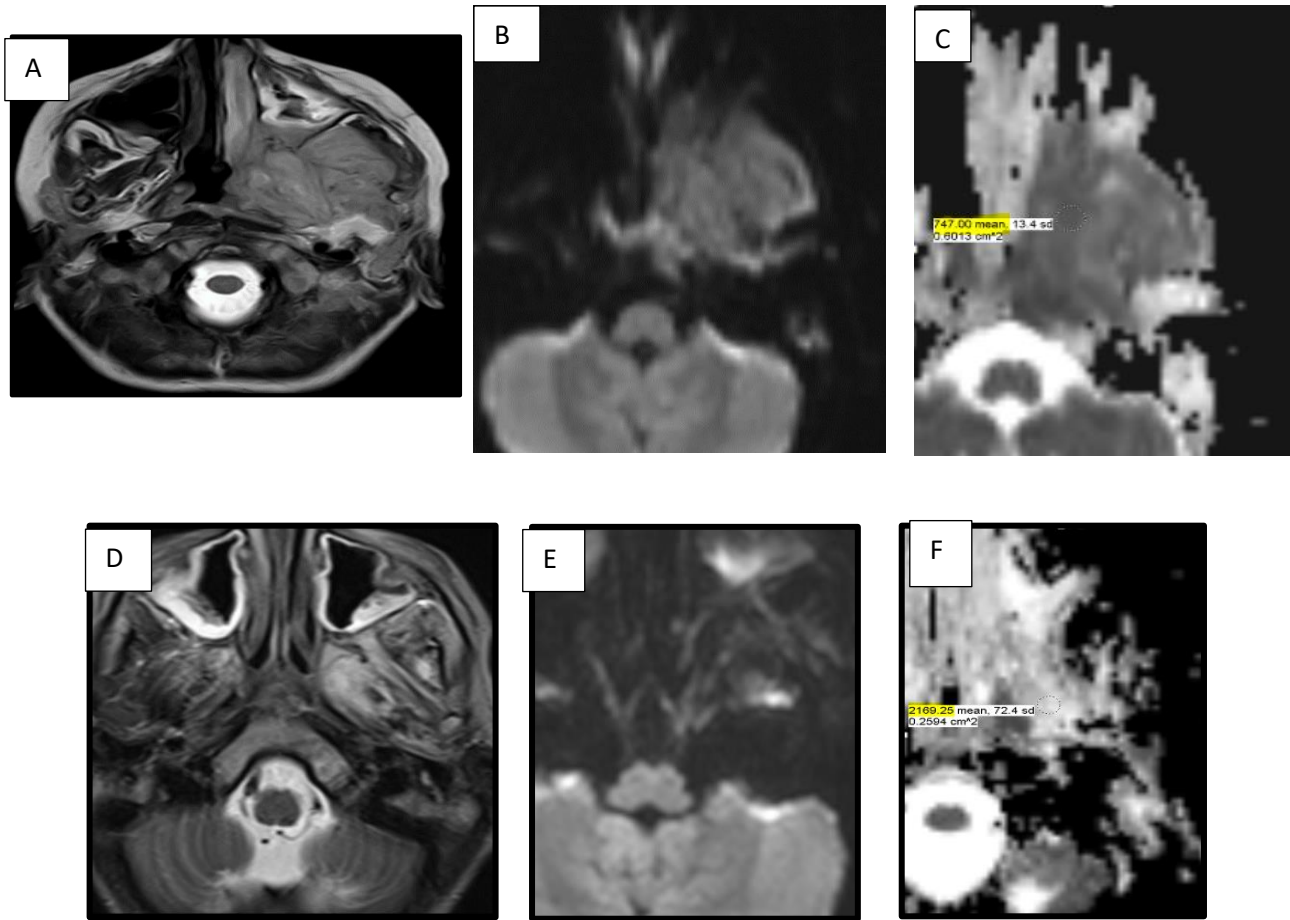


**Fig. 2: Left infratemporal Rhabdomyosarcoma in a 7-year-old male.**

- A. axial T2, B. axial MR DWI and C. ADC map images obtained prior to treatment show left infratemporal mass of low signal intensity that corresponds to a cellular tumor with ADC values of  $0.74 \times 10^{-3} \text{ mm}^2 / \text{sec}$ .
- D. axial T2, E. axial MR DWI and F. ADC map images obtained following treatment show area of architecture distortion with increase in signal heterogeneity and ADC values of  $2.1 \times 10^{-3} \text{ mm}^2 / \text{sec}$  that are consistent with post-therapeutic changes.
- The final PET/CT results show no uptake.

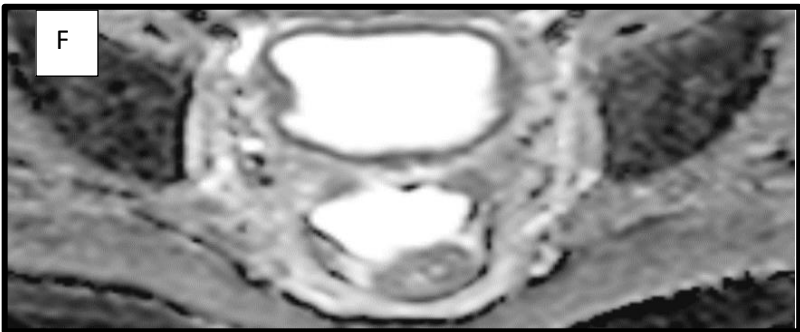
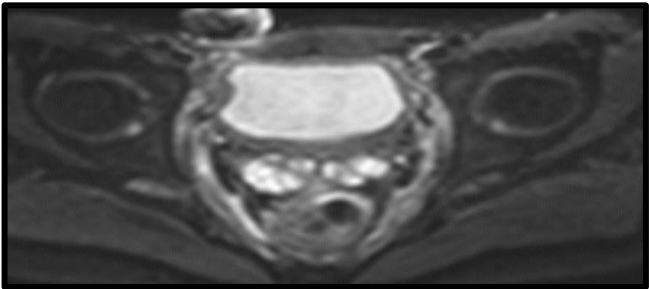
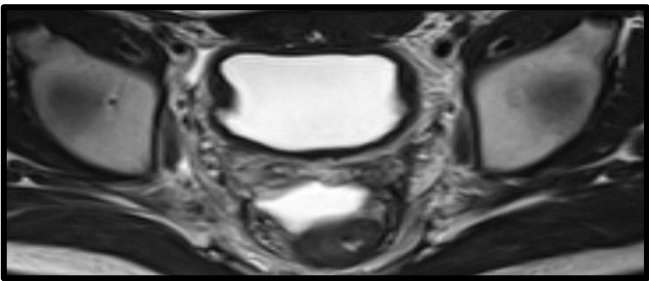
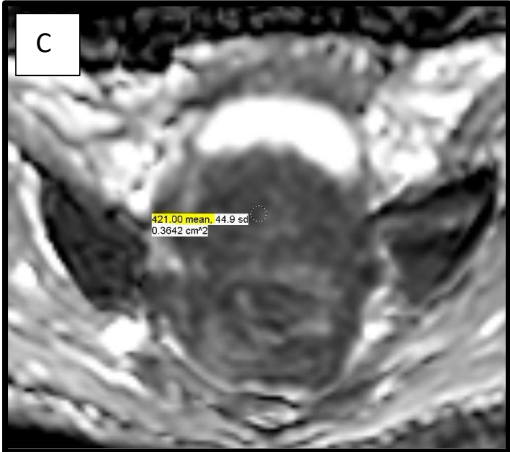
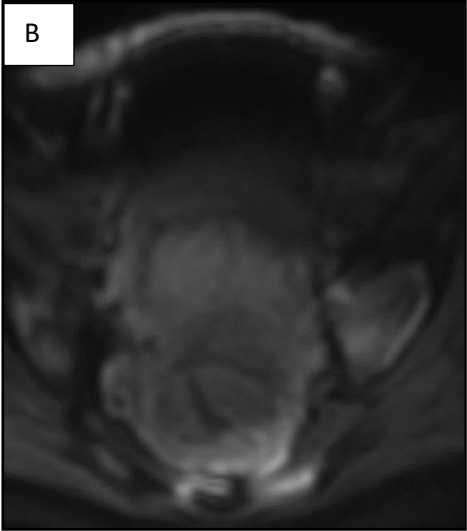
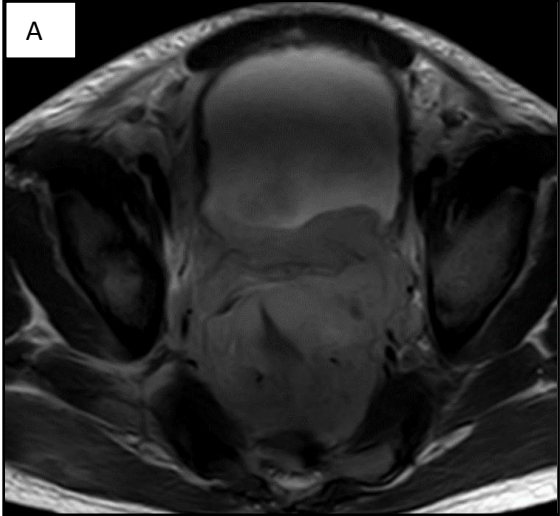


**Fig. 3: Pelvis Rhabdomyosarcoma in a 15-year-old male.**

- A. axial T2, B. axial MR DWI and C. ADC map images obtained prior to treatment show pelvic mass of low signal intensity that corresponds to a cellular tumor with ADC values of  $0.42 \times 10^{-3} \text{ mm}^2/\text{sec}$ .
- D. axial T2, E. axial MR DWI and F. ADC map images obtained at end of treatment shows no area of restricted diffusion with no residual lesion.
- The final PET/CT results show no uptake.

## Conclusion:

The DWI and ADC can assist in the evaluation of RMS and are used as markers to assess tumor response as well as differentiation between recurrent tumor and post-therapeutic changes.

## List of abbreviation

(MRI) magnetic resonance imaging, (DWI) diffusion-weighted imaging, (ADC) apparent diffusion coefficient, (RMS) rhabdomyosarcoma, (PET/CT) Positron emission tomography/Computerized tomography, (SUV/MAX) Standardized uptake value/maximum, (eRMS) Embryonal Rhabdomyosarcoma., (CEMRI) Contrast-enhanced magnetic resonance imaging, (T) Tesla, (TFE) Turbo field echo, (DTPA) Diethylenetriamine penta-acetic acid, (TR) Repetition time, (TE) Echo time, (NEX) Number of excitations, (ROI) Region of interest, (HNRMS) Head and neck rhabdomyosarcoma, (ARMS) Alveolar Rhabdomyosarcoma, (PRMS) Pleomorphic Rhabdomyosarcoma .

## References:

1. Salem B , Hofherr S, Turner J, Doros L, Smpokou P. Childhood Rhabdomyosarcoma in Association with a RASopathy Clinical Phenotype and Mosaic Germline SOS1 Duplication. *J Pediatr Hematol Oncol.*(2016) Nov;38(8):e278-e282.
2. L. A. Fowkes, D.-M. Koh, D. MacVicar, D. Levine, J. Chisholm. CT and MRI imaging

features of paediatric rhabdomyosarcomas (RMS). (2016)10.1594/ecr2016/C-1441

3. Nicole J. M. Freling, Rick R. van Rijn, Peerooz Saeed, Johannes H M Merks, Alfons J M Balm, Bradley R Pieters, et al. Imaging findings in craniofacial childhood rhabdomyosarcoma *PediatricRadiol* (2010) 40:1723–1738.
4. J. HalaburdaBerni, I. Delgado, A. Sánchez-Montañez, E. Vazquez, S. Gallego Melcon. MR Imaging Findings In Pediatric Head And Neck Rhabdomyosarcoma (2014)10.1594/ecr2014/C-1990.
5. Harriet C. Diffusion-weighted MRI in head and neck radiology: applications in oncology. *Cancer Imaging* (2010) 10, 209\_214.
6. Zbaeren P, Tshering Vogel DW, Thoeny HC. Cancer of the oral Cavity and oropharynx. *Cancer Imaging* (2010) 16: 62\_72.
7. Khoo MM, Tyler PA, Saifuddin A, Padhani A. Diffusion-weighted imaging (DWI) in musculoskeletal MRI: a critical review. *Skeletal Radiology*, 40(6), 665–81.
8. Owosho A, Huang S, Chen S, Kashikar S, Estilo C, Wolden , et al. A clinicopathologic study of head and neck rhabdomyosarcomas showing FOXO1 fusion-positive alveolar and MYOD1-mutant sclerosing are associated with unfavorable outcome. *Oral Oncol* 2016, 61:89-97.
9. Iatrou I, Schoinohoriti O, Tzermpos F, Theologie-Lygidakis N, Vessala A. Rhabdomyosarcoma of the maxillofacial



- region in children and adolescents: Report of 9 cases and literature review. *J Craniomaxillofac Surg* 2017; 45: 831–8.
10. Vilanova JC, Parizel PM, Gielen JL, Vanhoenacker F, Rijswijk C, Krestan C, et al. WHO Classification of Soft Tissue Tumors. Imaging of Soft Tissue Tumors. Heidelberg, Germany: Springer, 2017; 187–196.
  11. Baleato S, Romero MJ, Luna A, Vilanove JC, Arranz JC. Assessment of Musculoskeletal Malignancies with Functional MR Imaging. *Magn Reson Imaging Clin N Am* 2016; 24(1):239–259.
  12. Hong JH, Jee WH, Jung CK, Jung JY, Shin SH, Chung YG. Soft tissue sarcoma: adding diffusion-weighted imaging improves MR imaging evaluation of tumor margin infiltration. *Eur Radiol* 2019;29(5):2589–2597.
  13. Kamitani T, Matsuo Y, Yabuuchi H, Fujita N, Nagao M, Jinnouchi M, et al. Correlations between apparent diffusion coefficient values and prognostic factors of breast Cancer. *Magn Reson Med Sci.* 2013;12(3):193–9.
  14. Meng Li, Xiuju Bian, Rui Jing, Aijun Zhang, Nianzheng Sun, Xiuli JU, et al. Retrospective analysis of rhabdomyosarcoma (RMS) in children in a single center. *Thoracic Cancer* 9 (2018) 1180–1184. doi: 10.1111/1759-7714.12823.
  15. Kim JR, Yoon HM, Koh KN, Jung AY. Rhabdomyosarcoma in Children and Adolescents: Patterns and Risk Factors of Distant Metastasis., *American Journal of Roentgenology.* 2017;209: 409-416.10.2214/AJR.16.17466.
  16. Khoo MM, Tyler PA, Saifuddin A, Padhani A. Diffusion-weighted imaging (DWI) in musculoskeletal MRI: a critical review. *Skeletal Radiology*, 40(6), 665–81.
  17. Kumar Y, Khaleel M, Boothe E, Awdeh H, Wadhwa V, Chhabra A. Role of diffusion weighted imaging in musculoskeletal infections: Current perspectives. *Eur Radiol* 2017; 27: 414–423.
  18. Albalawi ED, Alkatan HM, Elkhamary SM, Safieh LA, Maktabi AM. “Genetic profiling of rhabdomyosarcomas with clinicopathological and radiological” *canadian journal of ophthalmology.* Volume 54, issue 2 April 2019, page 247-257.
  19. Norman G, Fayer D, McHugh K, Light K, McHugh K, Levine D, et al. Mind the gap: extent of use of diffusion-weighted MRI in children with rhabdomyosarcoma. *Pediatr Radiol* 2015;45(5):778–781.
  20. Humphries PD, Sebire NJ, Siegel MJ, Olsen OE. Tumors in Pediatric Patients at Diffusion-weighted MR Imaging: Apparent Diffusion Coefficient and Tumor Cellularity *Pediatr Radiol* 2007;36:857–859.
  21. Vermoolen MA, Kwee TC, Nievelstein RA. Apparent diffusion coefficient measurements in the differentiation between benign and malignant lesions: a systematic review. *Insights Imaging* (2012) 3:395–409.
  22. Hassold N, Warmuth-Metz M, Winkler B, Kreissl M, Ernestus K, Beer M, et al. “Hit the mark with diffusion-weighted MRI: metastases of rhabdomyosarcomas to the extraocular eye muscles” *BMC pediatric*, 2014; 14:57.
  23. Del Grande F, Subhawong T, Weber K, Aro M, Muger C, Fayad L. Detection of Soft-Tissue Sarcoma Recurrence: Added Value of Functional MR Imaging Techniques at 3.0 T. 2014; 271 (2):499–511.
  24. Ashkan A, Michael A, Riham H, Atif Z, Celia P, Katarzyna J, et al. Principles and Applications of Diffusion-weighted Imaging in Cancer Detection, Staging, and Treatment Follow-up. *RadioGraphics* 2011; 31:1773–1791.

**To cite this article:** Rehab Ibraheem, Medhat Refaat, Inas M. El-nadi , Tarek A. Raafat. Role of MRI Diffusion in Evaluation the Therapeutic Response and Prognostic Outcome in Pediatric Patients with Rhabdomyosarcoma. *BMFJ* 2022; 39 (Radiology):286-302. DOI: 10.21608/bmfj.2021.84481.1440